Tarnish Phenomena of Silver: Chemical Interactions, Analysis Methods and Real-Life Estimation

1. Abstract

The knowledge and the current testing methods regarding silver tarnish phenomena are not guaranteed to provide measurable evaluations of the phenomenon itself. Presently, all the formal and suggested tests are unable to demonstrate with any certainty what actually occurs, and they are especially unable to provide objective data. In fact, the tests are always carried out using a parallel reference sample, and so, provide only viewable, empirical data. Furthermore, the assumption is that once a minimum change in the test conditions takes place, the results become completely distorted. By following a more scientific method this paper will investigate more deeply into our knowledge of the chemical interactions that provoke the tarnish phenomena. The goal is to provide more trustworthy and repeatable data.

2. Introduction

The main aim of jewelry is its aesthetical features, which are greatly diminished when the bright, shining and sparking metal surfaces undergo corrosion, altering the color and the brightness. In the case of gold alloys this problem is displayed only after a long time and even then it is less perceptible, but silver can tarnish quite rapidly and sometimes the luster is lost before the item reaches the final user. Even though silver tarnish is a very important problem, it seems we do not have exhaustive knowledge of it. While the consequences of tarnish are very well known, the same cannot be said for the causes or the mechanisms. Also lacking is an adequate method for objective evaluation to give measure for the effects considered.

This paper has as its final aim to add some tessera to help and decipher the whole outline of the phenomena. The corrosion sustained by the surfaces of the items is mainly due to the direct contact with the external environment, where chemical agents can be dispersed and are able to induce oxide-reductive reactions on the surface of the material. Such reactions are therefore responsible for the growth of compounds on the metal that modify the optical reflection properties of its surface. Particular attention was paid to the chemical and metallurgic factors that play a fundamental role in silver tarnish. In the bibliography you can find several studies which describe the darkening process of silver as a result of a chemical reaction with aggressive agents such as sulfur (or its compounds), oxygen or chlorine, in presence of enough high relative humidity values. In our daily routine all these chemical agents are working together to attack silver, thanks to a complex system of reactions. In order to set adequate methods for each one of these trials in the research, we carried out separate sulfuration tests, high-temperature oxidation tests and tests which exposed the samples to light radiation. At the same time, the necessity to do an objective measurement of the above-mentioned results was developed, as will be shown.

3. Chemical reactions between Silver and Sulfur (and its compounds)

Historically, tarnish reactions were identified mainly as reactions between silver and sulfur. These take place at room temperature and are correlated (even if not in an universal manner) to reactions where the aggressive agent is oxygen. In literature, several studies demonstrated that the sulfur is mainly responsible for this phenomenon, under the influence of hydrogen sulfide. Simply, the reaction between silver and sulfur leads to the growth of silver sulfide according to the following reaction:

$$2\,Ag(s) + H_2S \rightarrow Ag_2S(S) + 2H^+ + 2e^- \qquad (1)$$

$$E = -0{,}03 - 0{,}059\,pH - 0{,}0295 \log P(H_2S)$$

The product of the reaction appears as a very well compact and typically yellowish to brownish superficial layer.

In truth, since hydrogen sulfide is a weak acid (Ka1 = 2.5*10-7; Ka2 = 1.6*10-14), it can be present in the atmosphere under a dissociated form and therefore, to the reaction previously seen we should add the following reactions:

$$2\,Ag(s) + HS^- \rightarrow Ag_2S(S) + H^+ + 2e^- \qquad (2)$$

$$E = -0{,}27 - 0{,}0295\ pH - 0{,}0295 \log a(HS^-)$$

$$2\,Ag(s) + S^{-2} \rightarrow Ag_2S(S) + 2e^- \qquad (3)$$

$$E = -0{,}68 - 0{,}0295 \log a(S^{-2})$$

$$Ag_2S(s) + H_2O \rightarrow Ag_2O(S) + S + 2H^+ + 2e^- \qquad (4)$$

$$E = 1{,}38 - 0{,}059\ pH$$

As you can see by the equations for the calculation of the potentials E, the reactions can be favored by some purposed variations of the pH together with some changes in temperatures that directly act on the thermodynamic parameters and on the concentrations of the reactants [1, 2]. Moreover, as reported in reaction (4), the presence of water may induce a further reaction of silver with the formation of Ag20.

In the presence of humidity a thin layer of water, physisorbated by the surface of the items, might promote tarnish connected to the presence of sulfur since it can induce the grouth of electrolytic microcells where you can have particular thermodynamic conditions, which determinate a high increased of the reaction rate. In addition, it should be taken into consideration that hydrogen sulfide has a discreet solubility in water and so the concentration of this acid in the atmosphere can be substantially different from what is really in contact with the surface of the metal as a film of water. The variation of humidity does not seem to have an appreciable effect of the average that silver sulfide film forms; however, the presumed function of humidity is to provide a preferential means for the transformation of the hydrogen sulfide into sulfide, and it aids the presence and mobility of these reactants on the surface of the metal. [3]

As already mentioned, sulfur (sulfides vapor) is the tarnish agent most significantly present in the earth's atmosphere. Sulfur is also present in compounds such as sulfhydryl compound, sulfates, sulfides and organic bisulfite, present in the environment as a result of natural processes and the anthropogenic activities, so mostly present in urban and industrial realities.

In conclusion, the only presence of polluting elements in the air is not enough to activate the reaction. Other determining factors, such as humidity and temperature, are in fact necessary. Especially, the presence of water in the thickness of some atomic layers absorbed by the surface of the metal plays the role to favor the kinetic of the reaction, acting as a preferential exchange interface for the reactants that take part in the corrosion process. In fact, a reaction that takes place in a watery environment displays minor activation energy when compared to the same reaction in a gaseous environment. Also, the presence of oxygen contributes to accelerating the reaction, and the temperature is favoring the kinetic.

The tarnish phenomenon displays like a process of multi-equilibriums, i.e., made of several concomitant chemical reactions and involving different corrosive agents, not all well known. This phenomenon is highly connected to the external environment and so the entity of the color variation of the silver items and the speed of growth of the tarnish film, should be analyzed by taking into consideration the environment where the phenomenon is observed.

4. Evaluation of the phenomena

As seen in the previous section, the formation of tarnish is favored by the presence in the atmosphere of sulfur or sulfur compounds and depends on environmental parameters such as relative humidity and the temperature. It is displayed as discoloration of the piece due to the formation of silver-based compounds on the surface. Physically, the formation of such compounds takes a variation of the original dielectric constant of the material surface. This constant, related to the chemical-structural characteristics of the material itself, rules the propagation of the light radiation in the material itself. In other words, the formation of the tarnish film modifies the ratio between reflectance and transmittance of the electromagnetic radiation that affects the material itself; therefore, such variation is perceived by the human eye as a variation of the color.

In the past, to quantify the tarnish phenomenon on silver items, several types of tests were set up. These were based on the use of sulfur-derivate compounds as hydrogen sulfide, sodium sulfide or thioacetamide (CH3CSNH2). The items put in contact with solutions, or vapors, containing such compounds display an evident color change in a short amount of time. Such test typologies were therefore called accelerated tests.

Our R&D Lab adopted the same type of tests to evaluate the resistance to tarnish of a silver alloy. They are very aggressive tests that in a very short amount of time can drive very evident tarnish discoloration, which would be totally unacceptable for an ornament. In face in our case, the yellowish color is already enough to reject the item. From here on, the necessity to set up a method which displayed a higher sensitivity during the first phases of the aggression, i.e., be able to perceive the minimum color toning of the surfaces, became fundamental. During this sulfuration test (in any case to be considered an accelerated test) you could detect the progression of color changes caused by tarnish with the naked eye as the samples were inspected at set and regular time intervals. The test therefore did not provide direct information on the real life estimation of the samples, but on the other hand, the results were used only as a direct comparison with a comparable material generally made of an alloy 92.5Ag7.5Cu. The trial was then interrupted when also the most resistant sample began to vary its own color.

Here following we report the method we set up, beginning from EN ISO4538: metallic coatings – Thioacetamide corrosion test (TAA test).

The reaction chamber consisted of a transparent glass desiccator with a watertight cover and a capacity of 11 liters. The test pieces were 28mm diameter disks. We produced a highly reactive atmosphere inside the chamber with a mixture containing 20μl of 20% ammonium sulfide in 120ml of de-ionized water. We used a non-ionic surface-active agent (Sodium Lauryl). We deposited 60ml of the prepared solution in the bottom of the desiccator. A 240mm diameter perforated porcelain plate was used to deliver evenly defused vapor to test pieces. This prevented the test pieces from directly touching the solution. We placed a 200mm clock glass at the center of the perforated plate and at the very end a rack to hold the sample. The temperature was kept constant at 20±5°C (68±9°F). We observed the samples and took note of the color changes every 10 minutes. The test had a total time of 40 minutes. The onset of color change and the speed of the tarnish evolution had to be precisely observed. During the test, the chamber could be opened, but only for the time needed to closely observe the samples. At the end of the test, the samples were removed from the chamber, washed using de-ionized water and dried with an air jet to stop the reaction from advancing. Furthermore, the sample could only be handled with clean tweezers and not touched with bare hands to avoid adversely influencing the test. It should be noted that this method did not keep the relative humidity and the sulfur concentration constant, although these parameters tended to saturate in about 40 minutes after chamber closure. The room temperature in the laboratory of 25°C (77°F) was considered to be constant for the whole duration of the test.

Following what is described above, we reported the color of the various samples after different times from the beginning of the test (for example, the straw yellow or intense yellow or brown, etc.) in order to compare the resistance to tarnish by color variation. After several trials, we understood that the use of such method to characterize the samples behavior is subjective and widely influenced by the human variable.

Due to the complexity of the phenomena, a visual evaluation and therefore a subjective one, might take to erroneous conclusions. The human eye is also not sensitive to small variations of color and brightness, and is able to perceive only a limited part of the entire spectrum band. Moreover, visual evaluation is influenced by several external factors such as variation of environmental light up and to the competence and sensitiveness of the visible perception of the operator. So it was determined that trustworthy results could only be achieved if objective and reproducible measurements could be obtained.

Naturally, our desire was to find a scientific method that allowed for the precise evaluation of the tarnish discoloration and therefore, a scientific instrument that could detect the minimum color variations was needed, such as a spectrophotometer. The spectrophotometer allows converting the reflectance spectrum (from 360nm to 780nm) into CIELab colorimetric coordinates with a resolution equal to 0,01% of reflectance. The analysis of the color variation due to the tarnish was done, thereby quantifying the variations of the colorimetric coordinates L*, a* e b*, calculated by the direct acquisition of the reflectance optical spectrum [2].

Three series of tests were carried out to evaluate the repeatability of the results and also the efficiency of the use of a spectrophotometer in this kind of tests. The samples prepared were 28 mm diameter disks with a composition as reported in the following Table1.

Sample	Ag (‰)	Cu (‰)	Zn (‰)	Si (‰)	Altri (‰)
1	930	70	-	-	-
2	1000	-	-	-	-
3*	930	70	-	-	-
4	930	43	10	2	15

*Copper - 930‰ Silver alloy with a surface deposit of Silver obtained by galvanic processes

Table 1 – Compositions of the alloys analyzed in millesimals (‰).

The various samples were prepared using pure elements that were pre-alloyed and then cast into an ingot mold at 1000°C (1832°F), followed by rolling and cutting.

To guarantee the highest surface homogeneity among the samples, we decided to do a mechanical polishing using a lapping machine. In fact, hand polishing would not grant the same surface finish for all the samples and this might dramatically influence the test result. A first reading was made with the colorimeter after the samples were washed with de-ionized water followed by an acetone rinse and drying. They were then placed in the reaction chamber (desiccator) where a diluted solution of ammonium sulfide was placed. At set intervals of 10, 20, 30 and 40 minutes, the samples were taken from the chamber to carry out the colorimetric analysis. In this way we succeeded in obtaining different sets of colorimetric coordinates for different moments of the tests. The colorimetric coordinates measured during the test were referenced to the beginning values measured for each sample undergoing the test, in order to calculate the variation.

The choice to insert four samples of different composition at the same time (reported in Table 1) in the reaction chamber and to take them out together was basically made to minimize the perturbations inside the chamber itself.
We especially aimed to:

- Maintain the most uniform surface-reactant adsorbed system;
- Eliminate the "waste-times" connected to the phenomenon of superficial chemisorbating;
- Obtain a trend which simulates at best the real kinetic of the tarnish reaction.

The trends of the changes of the coordinates Δa* and Δb* and the luminosity ΔL* are reported, in absolute value, in the graphs of Figures 1, 2 and 4.

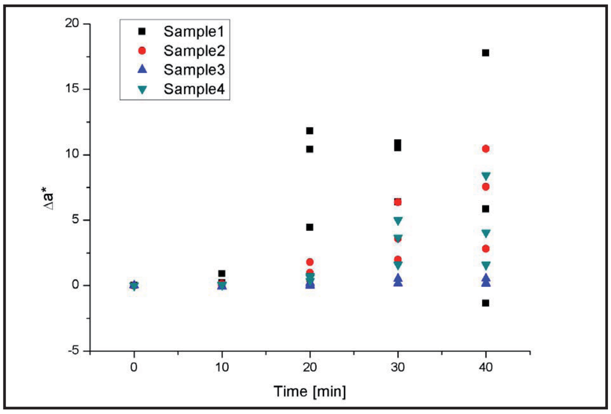

Figure 1 - Values Δa* detected by the sulfuration test.

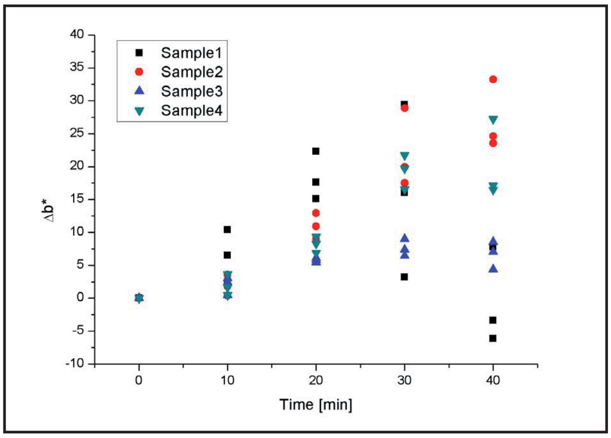

Figure 2 - Values Δb* detected by the sulfuration test

The values Δa* and Δb* display a rising trend almost until the end of the test, but in the last minutes it seems they suffer a regression. In truth it is an effect deriving from the theory on which the colorimetric space is built. Each one of the two coordinates (a* and b*) represents two colors: green and red for the coordinate a*, blue and yellow for the coordinate b* (see Figure 3). An increase, for example of the coordinate b*, represents a coloration towards yellow, while a reduction of the coordinate b* represents a coloration towards blue. This is why, in the first phases of the test, when the samples begin to turn yellow, you can notice a marked increase of b* coordinate, while at the same time a* increases a little, giving a color that, as time goes by, tends to reddish. So by analyzing the trends of Δa* and Δb* it is normal to see a reduction of such parameters, even if the reaction is still in progress.

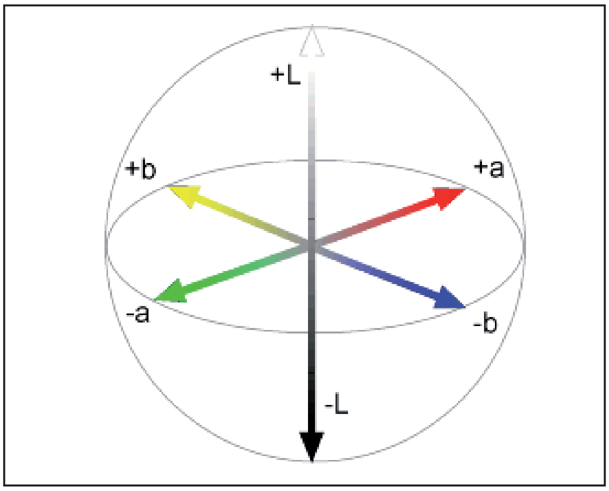

Figure3 – View of the colorimetric space defined by the coordinates L*, a* e b*.

A parameter that displays a monotonous trend throughout the test long is ΔL*. It represents a variation of luminosity, i.e., the quantity of light reflected by the samples. This is due to the opaque nature of the surface, as you can notice in Figure 4.
One of the aims of this job to correlate the general trend of the reaction to a unique parameter to quantify the spectrum variation of the sample itself. Even though ΔL* has a trend which might be traced back directly to a physical phenomenon, it does not take into consideration the color change on the plane a* b*. It should also be noted how the dispersion of data is increasing with the increased time of exposure to an aggressive environment.
This can be explained due to the fact that once the first yellowish film uniformly covered the samples, the reaction proceeds in a more inhomogeneous manner. In fact, some reddish spots begin to appear on the surface of the samples, and they tend to grow until covering the whole surface. This is evident especially in Sample 1, i.e., the sample with the higher trend to form superficial spots. As you can notice in Figures 1, 2 and 4, Δa* and Δb* are the parameters mostly involved by this dispersion, while ΔL* is less influenced, since it is related to the quantity of light reflected. This aspect, together with the handiness

of a unique parameter, led us to use ΔE as a term of comparison. Its mathematical definition is the following:

$$\Delta E = \sqrt{\left(\Delta L^{*2} + \Delta a^{*2} + \Delta b^{*2}\right)} \tag{5}$$

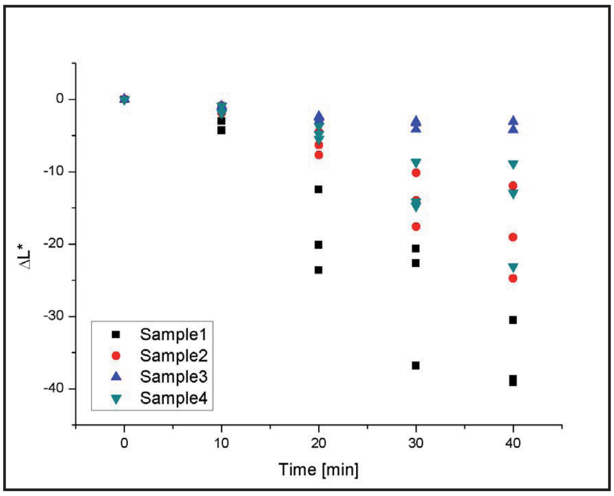

Figure 4 - Values ΔL* detected by the sulfuration test.

In small words, ΔE represents the length of the vector of the colorimetric movement in the color space. Its increase is directly and contemporaneously correlated to the color and luminosity variation of the sample. As a consequence, the higher its value, the higher the reaction of the sample will be with the external environment. Moreover, it represents a minor data dispersion for a long amount of time if compared to the one detected for Δa* and Δb* (see Figure 5).

While analyzing the data, we thought also of using spectrum curves obtained with the help of the colorimeter as a further source of information to quantify the tarnish phenomena. However, the variation of the reflectance curves does not involve the whole optical spectrum analyzed and so it is difficult to correlate the growth of the tarnish film with a unique spectrum wave length. Therefore, the study of these curves does not add any more details to those already provided by the analysis of the colorimetric coordinates and for that reason we report here only one example related to Sample 4 just to complete the information (Figure 6).

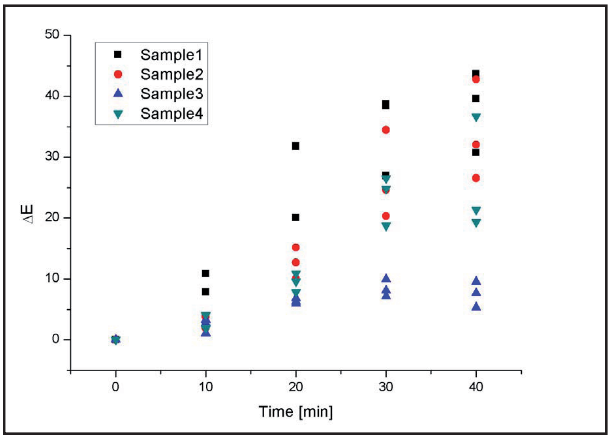

Figura 5 – Valori ΔE rilevati nel test di solfurazione

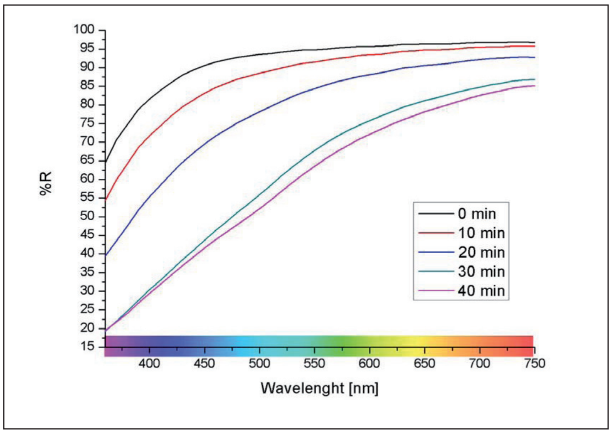

Figura 6 – Curve spettrali relative a Sample4 per il test di solfurazione

5. Damage induced by light radiation

The idea for this part of the job was actually given by daily routine. It is pretty common that the pieces made of silver alloy that stay tarnish-free for a very long time, once placed in a shop window, begin to tarnish in a few days' time. Light can cause significant damage for many different types of materials. This process can degrade the physical appearance and aesthetic appeal of silver, due to a loss of brightness and discoloration on the surface of the pieces themselves.

It is possible to divide electromagnetic spectrum into ultraviolet (UV), visible light (Vis) and infrared (IR). The wave length of infrared radiation is higher than 760nm, while the wave length of ultraviolet light is less than 400nm. Visible light can be perceived with the naked eye and its wave length falls between IR and UV light. To understand how the electromagnetic radiation might provoke photo-degradation phenomenon on the various types on sub-layers, we should take into consideration the quantum theory and chemical interaction. Briefly, we can explain the phenomenon by saying that the incident radiation, if absorbed by the material, might induce (with suitable limitations, ruled by precise selection rules) transactions among the different electronic levels of the atoms or the molecules composing the material. In case of UV-Vis radiations, these transactions especially involve the molecular orbitals of unsaturated or aromatic substances, or atoms with electronic doublets available. Light radiation of higher energy (UV) might also provoke scissions among the chemical bonds inside the molecules themselves, since the energy associated with such electromagnetic waves is comparable to the energy possessed by the chemical bond itself. Instead, the radiations with wave lengths that fall into the visible spectrum generally provoke the passage of electrons from a fundamental stage to an excited one, i.e., a redistribution of the electronic population among the various energetic levels of the atoms or the molecules making up the material.

The absorption of the IR radiations, characterized by a minor energetic content if compared to the visible radiations, causes instead transactions among the vibration stages of the molecules taking to stretching or bending incident of the chemical bonds. It should be remembered that the infrared spectrum of a molecule depends on two factors, the mass of the atoms bonded and the rigidity of the bond, and this is characteristic of each single chemical compound. The increase of vibration energy of the molecule induced by the absorption of infrared radiations also causes an increase of temperature of the system itself.

This brief explanation is helpful for the reader to know how the light radiation absorbed by a material might induce energetic variations of the atoms and molecules constituting the material itself in ways that are in function of the energy associated to the electromagnetic radiation. The absorption of a determinate light radiation is strictly correlated to the chemical structure of the material and can therefore favor, through the absorption of energy, the occurrence of determinate chemical reactions causing some macroscopic chemical-physical modifications of the structure of the material. The higher the absorbed energy (UV radiations) of the photon, the higher is the chance for electronic transactions associated with breaking the chemical bond. This takes place also with radiations that fall into the infrared spectrum, but with a different mechanism, since the increase of temperatures associated with the absorption of the IR radiations involves a reduction of the activation energy of the chemical reactions (thermal degradation). According to this, it is possible to think that the absorption of the IR radiations work as a “catalyst” for chemical processes photo-assisted by radiations of higher energy, for example UV radiations. The sunlight, which commonly heats us, is made essentially of wave lengths higher than 300nm, so it includes the region from ultraviolet to infrared. The ultraviolet spectrum can be divided into close UV (380-200 nm) and far UV (200-10 nm). The range of the UV wave lengths is further divided into UV-A (400-315 nm), UV-B (315-280 nm) and UV-C (280-10 nm). The sun gives off very intense radiations in the UV-A and UV-B spectrum, but this is absorbed by oxygen and ozone present in the stratosphere. These molecules constitute a natural shield against the noxious action of these ultraviolet rays.

The study of the photo-degradation activity induced by light radiation can be interesting, if you consider that silver items on display in shop windows are exposed for long periods to different systems of illumination (direct sunlight, incandescence lamps, fluorescents lamps etc.). At the same time, the light radiation is increasing the reactivity of the polluting agents present in the atmosphere and in contact with the silver items.

To quantify the photo-degradation experience induced by light radiations on silver in shop windows, it is necessary to choose a light source as a reference. Due to the different types of light sources available on the market (incandescence lamps, fluorescents lamps, mercury vapors lamps etc), a good choice seems to be a Xenon lamp. The spectrum of emission of this lamp contains all the spectrum of the lamps commonly employed and simulates the spectrum of sunlight very well (with the use of specific filters). The spectrum of this lamp contains variations of wave length higher than 290nm. The spectrum width covers therefore a range that goes from UV radiations to those falling close to IR.

6. Ageing test by light radiation

To simulate the behavior of silver items in the shops windows and to evaluate an eventual connection between light radiation and the superficial tarnish event, we decided to proceed with a series of tests where silver items underwent high intensity light radiations. This sort of test is used especially in the polymeric materials and the leather tanning industries to evaluate the resistance to light of those products and they are well known as ageing tests or Xenotest. Xenon lamp test chambers equipped for the control of incident light radiation intensity and temperature are used for this type of test. Tests made with the help of such instrument allow accelerated simulation of damage produced on items after a long exposure to direct sunlight. Moreover, ASTM and ISO standard are applied to such tests made on materials such as polymeric films, paints, clothing and leathers. The same four alloys analyzed during the sulfuration test underwent the Xenotest; of course a similar process was used to prepare the samples. We think in fact that the presence of a light radiation could indirectly influence the kinetic of these reactions, favoring the formation of superficial deposits responsible for the tarnish discoloration on silver items. The disks were lapped to a uniform high polish. The samples were then washed using de-ionized water and acetone and dried before colorimetric analysis was done.

Figure 7 –The instrument Q-Sun Xe1B used for the ageing tests.

After a series of trials at different energies, aimed to understand the function of the instrument and establish suitable parameters for our test, we settled on an irradiation intensity generated by a Xenon lamp of 1,4 kW/m2. The intensity of irradiation is measured with a radiometer set at a wave length of 420nm. A “daylight filter” was used between the lamp and the samples to simulate the spectrum of direct sunlight. The sun constant is the quantity of radiation reaching the earth for unit of surface, measured on a plane perpendicular to the rays at the earth’s upper atmosphere. The most recent measurements made with the help of satellites supply a value of 1366 W/m^2. This enormous quantity of energy does not entirely reach the earth’s surface. In fact 40% of the radiation is absorbed or reflected by the clouds and 15% is absorbed by the air; so only 45% reaches the ground. As a consequence, the choice to use a radiation equal to 1,4 kW/m2 represents the worst condition possible.

The instrument allows also temperature control inside the chamber by a sensor called a “Black Body Panel”. The temperature as measured on the “Black Body Panel” was kept constant at 60°C (140°F) for the duration of the test. The temperature control in the chamber is precise even though there is a slight difference between the black body and the samples due to their different thermal properties. To guarantee a constant temperature, the instrument is equipped with forced ventilation by dissipating heat generated by the Xenon lamp with room air and keeping the temperature of the black panel constant. However, it should be taken into consideration that the sensor is a black body and due to this, it absorbs all the radiation hitting it, while the samples would reflect some portion of the radiation hitting them and therefore absorb less energy and not bbe quite as hot.

The test made in our lab lasted 96 hours. During this period of time, the samples underwent a daily colorimetric analysis to evaluate the color variations. According to the results obtained with the sulfuration trials, we decided in this case to evaluate only the variations of the L* coordinate, carrying out an analysis on the vectorial motion of this coordinate (Figure 8). We also took the value of ΔE into consideration as a significant parameter (Figure 9).

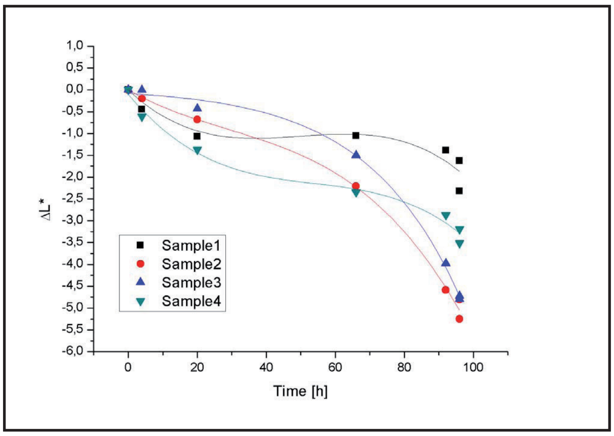

Figure 8 - Value ΔL* detected during Xenotest.

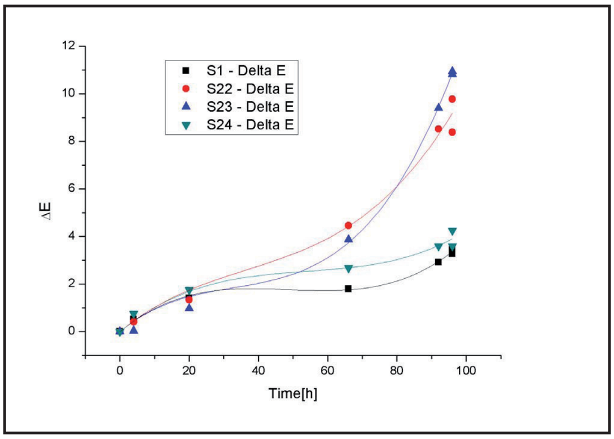

Figure 9 - Values ΔE detected during Xenotest.

As you see in Figures 8 and 9, the samples exposed to Xenotest might be distinctly divided into two families: samples with a pure metal surface (Sample 2 and 3) and samples made of alloy (Sample 1 and 4). The alloy samples probably evidenced a higher resistance to this ageing test due to the less silver concentration on the surface. This trend becomes evident in tests lasting more than 60 hours. To give a better idea of the difference, it is necessary to note that ΔE for less than 4-5 units hour is hardly perceptible to the naked eye. So this can be considered the limit at which an item is understood to have a color still aesthetically acceptable. The curves elaborating the data collected display complex trends that are well-suited to describe the kinetic of more concomitants reactions.

7. Oxidation at high temperature

Even though jewelry items are not subjected to high temperature oxidation during their daily use, high temperatures are a common part of the production phases. We decided to explore this aspect to complete and improve the knowledge of another type of corrosion phenomenon and to characterize the whole behavior of the items made of silver alloy. Usually the items made of silver alloy are not particularly subjected to oxidation phenomenon at environmental temperature. Silver, being a noble metal, displays low affinity to oxygen in normal use conditions. Even at high temperatures (T>200°C or >392°F), silver keeps its high resistance against oxygen, but since there is the presence of alloying elements in sterling silver alloys, the heat increases the kinetic of oxidation of the other elements. Therefore, the result is the formation of a layer of oxide on the surface of the items. A practical example may be the one of a traditional 93Ag7Cu alloy. When the items produced with this alloy have to undergo heat treatments at high temperature (700°C or 1292°C) during the production phase, they will be covered by a thick and dark copper oxide layer. Taking this as a clue, we decided to exactly simulate the process in question.

For this test we used the same four samples as per the composition reported in Table 1, prepared in the same way. The samples were put in a muffle kiln and extracted at pre-set time intervals for observation at the SEM microscope. We observed the samples before being put in the kiln and after 5, 30, 60, 120, 240 and 360 of heat treatment. In the case of oxidation at high temperature, we did not take colorimeter measurements because a dark oxide layer was formed more or less instantaneously or did not happen at all. The difference in behavior of the four samples can be appreciated by comparing the pictures displayed in Figure 10.

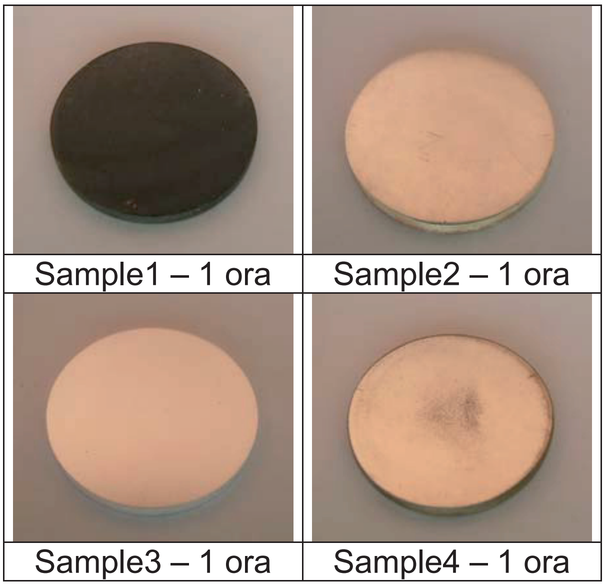
Sample1 – 1 ora
Sample2 – 1 ora
Sample3 – 1 ora
Sample4 – 1 ora

Figura 10 – Campioni dopo prova di ossidazione ad elevata temperatura (700°C per 1 ora)

I campioni 2 e 3 che presentavano una superficie composta di argento puro, come previsto, non hanno subito variazioni di colore, se non una leggera perdita di brillantezza. Anche il campione 1, lega Ag/Cu tradizionale, si è comportato come previsto, ovvero ossidandosi immediatamente una volta posto ad alta temperatura. Si può invece considerare positivamente anomalo il comportamento del campione Sample4. Trattandosi infatti di una lega a base Ag/Cu, poteva essere preventivabile una marcata ossidazione del rame con conseguente annerimento della superficie. Anche dopo 6 ore di test, invece, la superficie ha subito solo una leggera opacizzazione, mostrando dunque un comportamento simile ai campioni 2 e 3.

La mancanza di una misurazione colorimetrica diretta ed il comportamento del campione 4 ci hanno spinto ad osservazioni approfondite di questo fenomeno tramite l'utilizzo di un SEM in modo ha acquisire maggiori informazioni riguardanti la morfologia e la composizione superficiale dei campioni.

8. SEM observations

Following are the images (Figures 11-17) obtained using the SEM microscope of the several samples:

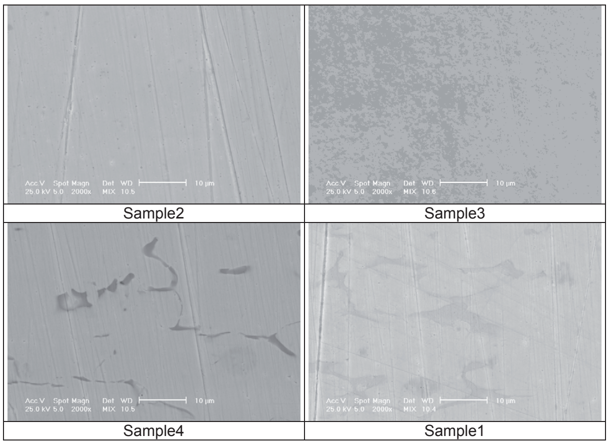
Sample2
Sample3
Sample4
Sample1

Figure 11 – SEM images of the 4 samples before the oxidation test

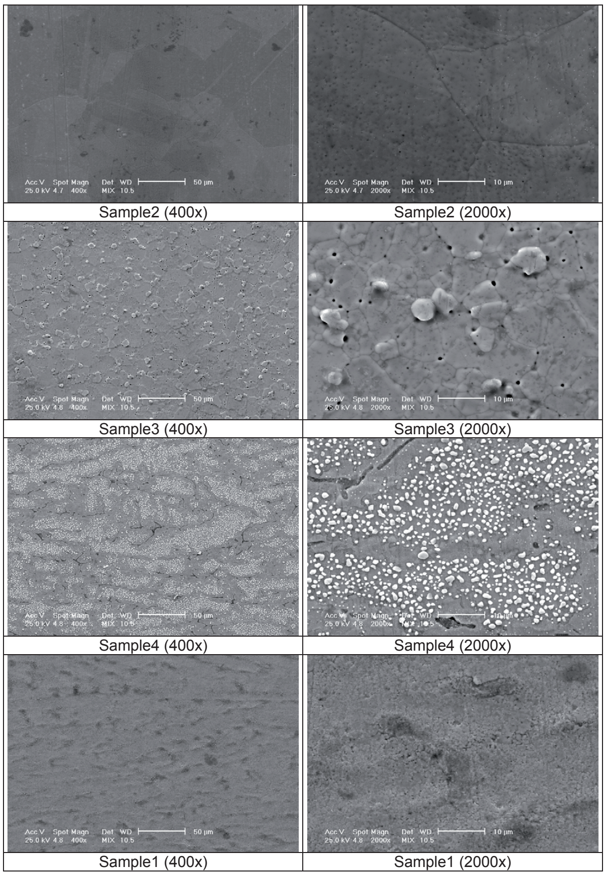

Sample2 (400x) Sample2 (2000x)

Sample3 (400x) Sample3 (2000x)

Sample4 (400x) Sample4 (2000x)

Sample1 (400x) Sample1 (2000x)

Figure 12 – SEM images of the 4 samples after 5 minutes at 700° (1292°F)

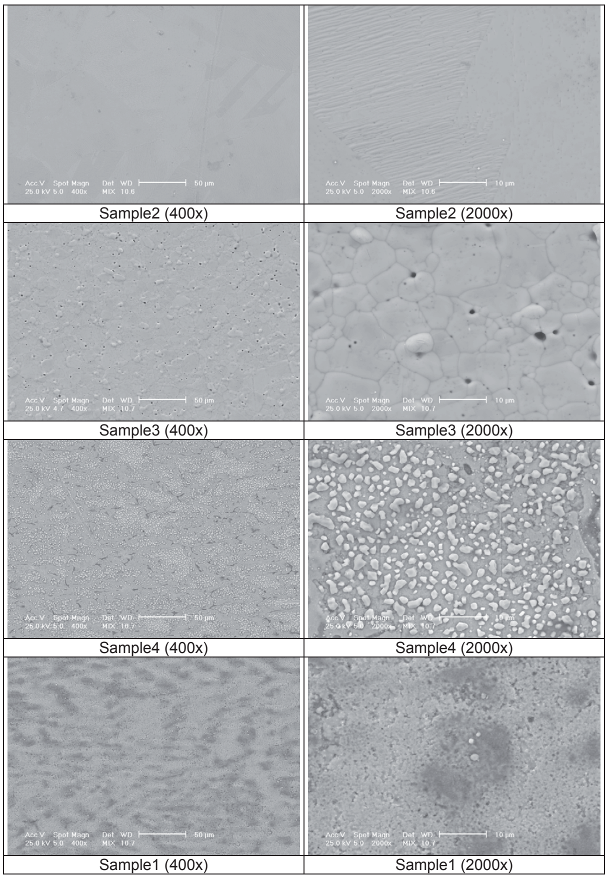

Sample2 (400x) Sample2 (2000x)

Sample3 (400x) Sample3 (2000x)

Sample4 (400x) Sample4 (2000x)

Sample1 (400x) Sample1 (2000x)

Figure 13 - SEM images of the 4 samples after 30 minutes at 700°C (1292°F)

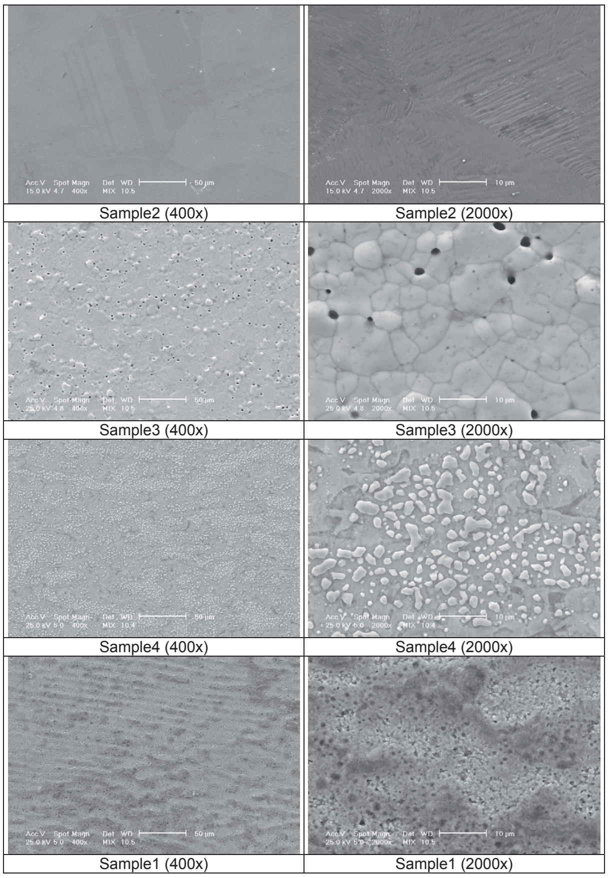

Sample2 (400x) Sample2 (2000x)

Sample3 (400x) Sample3 (2000x)

Sample4 (400x) Sample4 (2000x)

Sample1 (400x) Sample1 (2000x)

Figure 14 – SEM images of the 4 samples after 60 minutes at 700°C (1292°F)

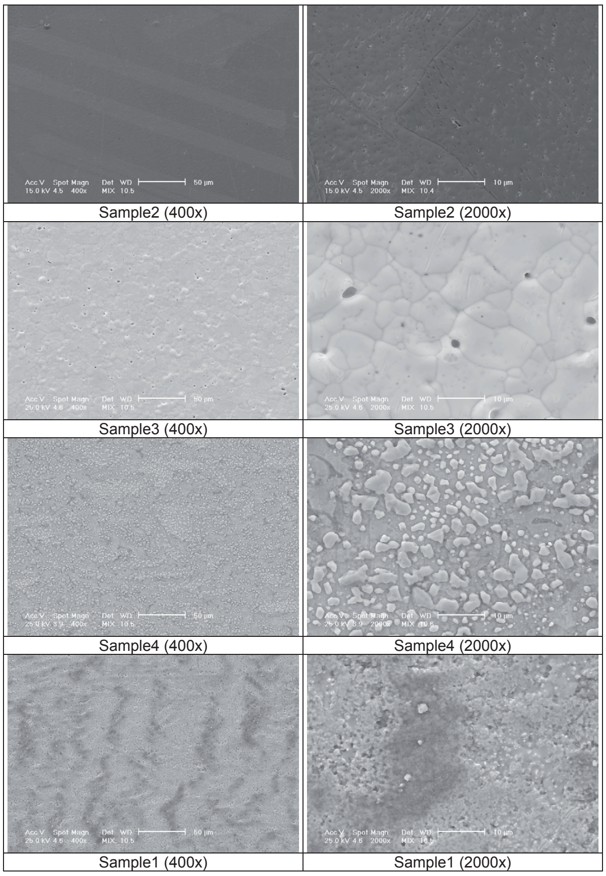

Sample2 (400x) Sample2 (2000x)

Sample3 (400x) Sample3 (2000x)

Sample4 (400x) Sample4 (2000x)

Sample1 (400x) Sample1 (2000x)

Figure 15 – SEM images of the 4 samples after 120 minutes at 700°C (1292°F)

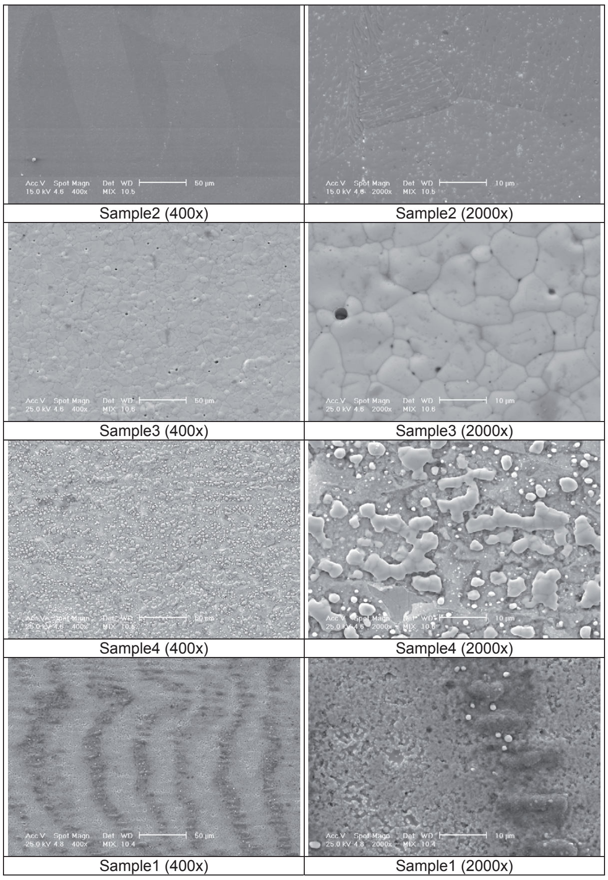
Sample2 (400x) Sample2 (2000x)
Sample3 (400x) Sample3 (2000x)
Sample4 (400x) Sample4 (2000x)
Sample1 (400x) Sample1 (2000x)

Figure 16 – SEM images of the 4 samples after 240 minutes at 700°C (1292°F)

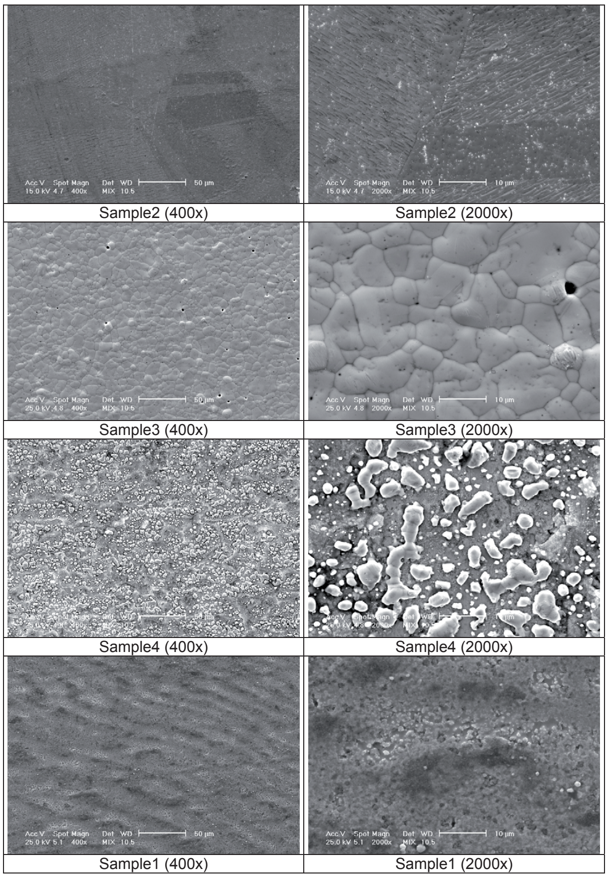
Sample2 (400x) Sample2 (2000x)
Sample3 (400x) Sample3 (2000x)
Sample4 (400x) Sample4 (2000x)
Sample1 (400x) Sample1 (2000x)

Figure 17 – SEM images of the 4 samples after 360 minutes at 700°C (1292°F)

As evidenced in the pictures show in Figures 11-17, the heat treatment causes a distinct crystalline pattern to be formed on the surface of Sample 2 that became progressively more distinct with increased heat treatment. In any case, even after 6 hours, despite a certain increase of the roughness (maybe responsible for the loss of reflection), the surface quality is still high.

The images of sample 3 show that after the first heat-treat period the surface suffered a higher degradation, with cavities forming and micro-roughness on the surface caused by the growth of raised crystalline grains that takes to elevate phenomena of micro-roughness on the surface itself. This phenomenon is due to the presence of defects in the superficial layer (almost 2µm) deposited by galvanic plating. Presumably the heat caused by micro-bubbles of gas to expand, creating the so-called porosity. The occurrence can be traced to the presence of galvanic bath additive residuals that remain embedded during the deposition of the metal. It is interesting that well-defined granular regions that were formed in the early stages of heat treatment become coalesced over time and the porosity caused by the explosion of gas bubbles is mostly repaired. Even in this case, apart from a certain increase in roughness, which creates light diffraction phenomenon, the surface quality is not compromised.

As expected, SEM analysis of Sample 1 shows the surface before the heat treatment has zones made of different composition (darker zones) where we found a higher presence of copper. This superficial microstructure is the result of micro-segregation typical of an alloy that generates a bi-phase structure. Even after only five minutes at high temperature, a noticeable oxide layer presents an irregular and porous surface that seems to get worse with extension of heat treatment time. The morphology of such film is totally compatible to the one of an oxide. In this case we noticed the dark grey copper oxide (II), and some red cuprite oxide areas, i.e., copper oxide (I).

Before being put into the muffle furnace, Sample 4 displayed a bi-phase surface very similar to Sample 1. However, after heat treatment the appearance is completely different. After 5 minutes it is possible to observe the growth of micro-zones, or islands of bright color surrounding the copper-rich zones. The microanalysis made on these points evidenced the presence of pure silver crystals. As the time spent into the furnace increased, these islands began to grow to the detriment of the copper-rich zones, followed by coalescence by the end of the heat treatment time. After 6 hours at 700°C (1292°F), you can no longer notice the presence of dark zones, and the many small islands of pure silver that are more widely spaced. It is our opinion that the high resistance to oxidation at high temperatures is in part due to this enrichment of silver on the surface of the sample.

According to the information collected by the SEM observations of the oxidized samples, we thought it was good to also extend our observation to the samples that underwent the sulfuration and Xenotest (Figure 18 and Figure 19).

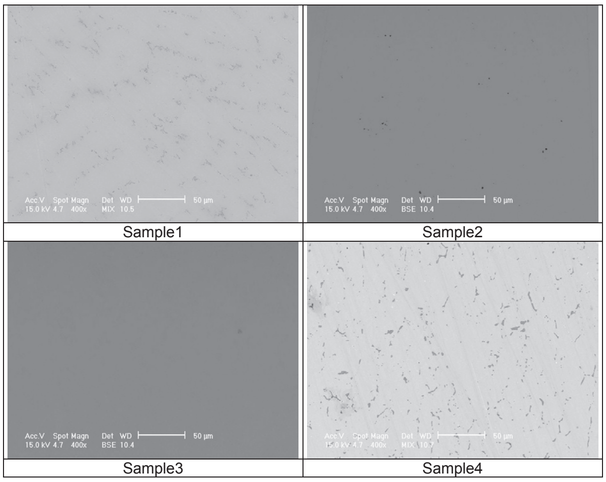
Sample1
Sample2
Sample3
Sample4

Figure 18 - SEM images of the 4 samples after sulfuration test (40 minutes)

The reaction products of tarnish are very thin and therefore little morphological or compositional information can be collected. However, observations made on the samples exposed to the Xenotest were applied to the sulfuration samples and we decided to report what we could.

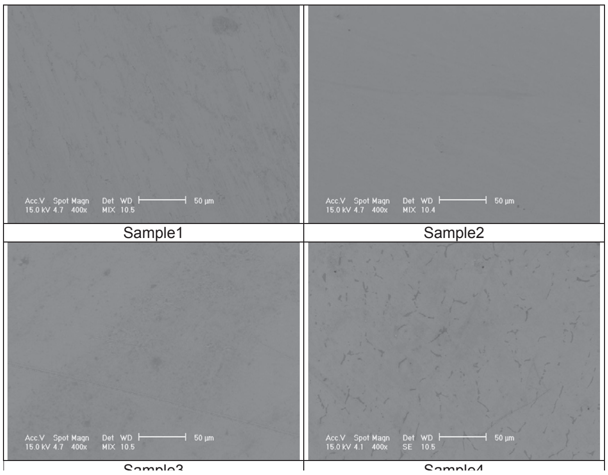
Sample1
Sample2
Sample3
Sample4

Figure 19 - SEM images of the 4 samples after Xenotest (96 hours)

9. Compositional superficial analysis

To correctly evaluate the data provided by different trials carried out at our Labs, it is important to fully understand the mechanism of corrosive film (tarnish film) growth, and therefore know the superficial composition of the different sample to compare them to the colorimetric data previously obtained. This correlation might allow us to understand the mechanism of the reactants that are taking part to the reaction, and allow us to estimate the tarnish film growth kinetics.

The technique used for the superficial compositional analysis is the GDOES (glow discharge optical emission spectroscopy) 4, 5. GDOES is a recently introduced technology that is still being optimized. It is a type of elemental spectroscopic analysis able to measure the concentration and depth of elements on the surface of a sample. The technique doest obtain data regarding chemical bonds or interactions among the atoms composing the superficial film. This destructive technique was developed for the study of thin films and nanotechnology coatings, since it allows you to analyze the concentration of different chemical elements in films with thickness varying from some nanometer to some tens of micrometers. The GDOES technique is based on rapid and uniform erosion on the surface of the test sample by argon plasma sputtering (Figures 20 and 21).

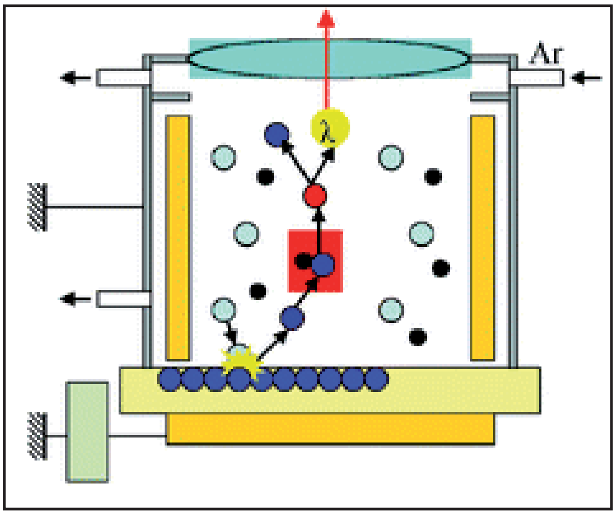

Figure 20 - Simplified sketch of the GDOES spectroscopy technique.

The plasma is confined in a chamber where the sample undergoing the analysis is the cathode on which a constant voltage is applied.
The plasma discharge developed between the sample and the anode is stabilized by optimizing some parameters such as the potential applied (between 600 and 900V) and the current generated (of some ten nA). These parameters allow maintaining a constant sputtering rate, which may vary between 500 and 700 nm/s. The plasma excites the atoms, or in some cases a small clusters of atoms, coming from the superficial erosion of the sample surface through a several collisions that they have with the particles in the plasma. The relaxing of the atoms at their fundamental stage is characterized by the optical emission typical of the atom itself and the intensity is proportional to its concentration. The electromagnetic radiation emitted is then detected by some photo-multipliers or, as an alternative, by some CCD sensors, and the signals are sent to

a computer program where they are converted to useable data. These devices are able to detect the element concentration profiles making up thin films with a good spatial resolution.

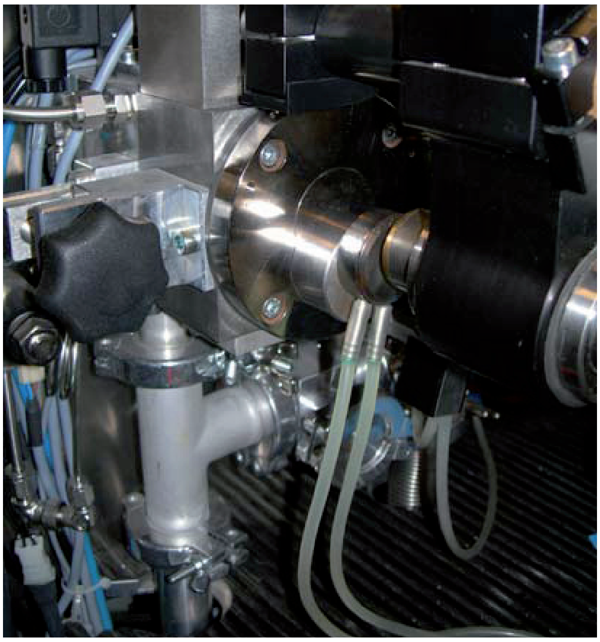

Figure 21 – Detail of GDOES instrument

According to the nature of the samples undergoing the analysis, it was not possible to obtain a quantitative analysis of the elements present on the samples, but semi-quantitative analysis can be obtained by comparisons. Since GDOES is still in development, calibration of the instrument for silver was not possible due to the lack of developed calibration curves. The samples undergoing the investigation are disks made of silver or silver alloy (Table 1) obtained by the procedure described in the previous sections and exposed to different corrosion tests.

Each of the four sample series of disks in Table 1 underwent threetests as follows:

- Sulfuration test: 40 minutes;
- Corrosion test at high temperature (700°C) : 6 hours;
- Ageing test (Xenotest) at 1,4kW/m2 at 60°C for 96 hours.

The different corrosion steps are reported below. The analysis of the samples was made by Dr. Simone Vezzù of CIVEN (Venetian Interuniversity Coordination for Nanotechnologies), Marghera, Venice. An additional set of sample disks (that were not subjected to the series of corrosion tests) was prepared to provide a baseline for the GDOES investigation.

An evaluation of the emission intensity of hydrogen, oxygen, copper, zinc, sulfur and silver was done with the GDOES to form a baseline using the Sample 1 set of disks. As you see from Graph 1, in the very first superficial atomic layers appreciable quantities of oxygen, hydrogen and sulfur are present. This sample was analyzed some days after polishing and it is possible that a thin layer formed on the surface of the sample, due to the reaction of the metal with sulfur or sulfur-derivates, and the humidity present in the surrounding environment.

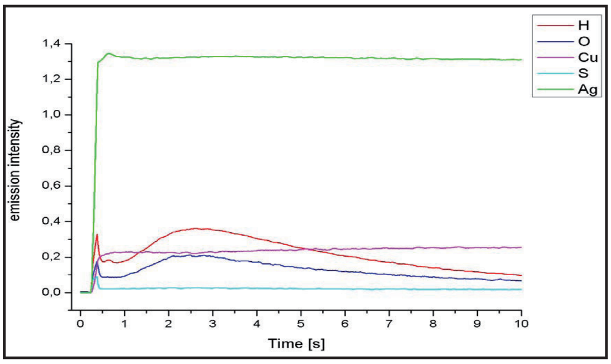

Graph 1 – GDOES analysis made on baseline samples

It is also possible the oxygen and hydrogen observed in the sub-superficial layer were diffused inside the sample during the annealing heat treatment or during the casting phase and preparation of the sample itself.

Sample 1 exposed to Xenotest (1,4kW, 60°C/140°F for 96 hours long) displays the presence of a sub-superficial layer almost similar to the one seen in Graph 1 (Graph 2).

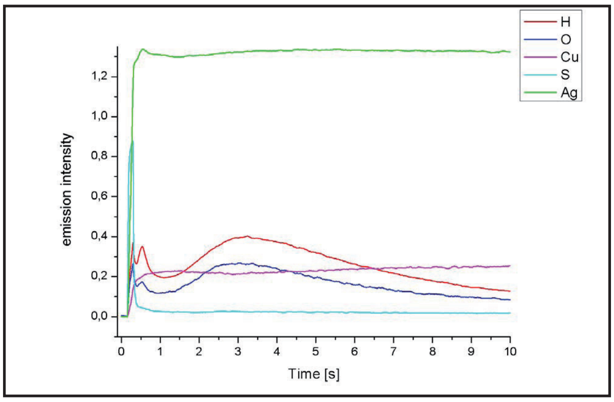

Graph 2 – GDOES analysis of sample 1 after Xenotest

The first superficial layers of this sample are reported in detail in Graph 3. You can see the superficial deposit of elements such as oxygen, hydrogen and sulfur which interact with the silver and copper of the sub-layer and how this layer developed, most probably on a humidity layer, as evidenced by the presence of some peaks of oxygen and hydrogen after around 0,6 seconds from the beginning of the analysis itself (on the right is the peak of sulfur).

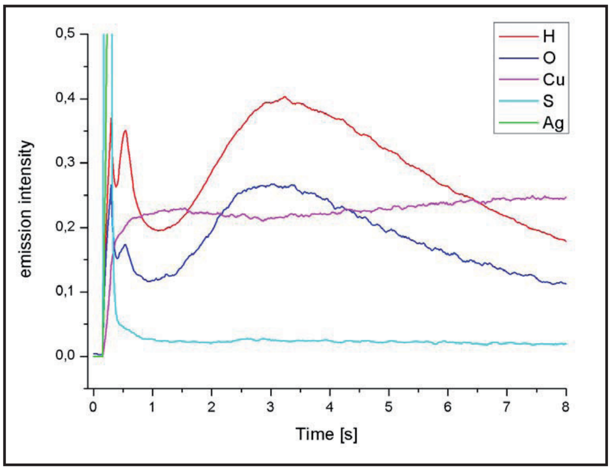

Graph 3 – Zoom of the GDOES analysis of Sample 1 after Xenotest

The sample exposed to an accelerated sulfuration test evidences, instead, a high content of sulfur in the first superficial layers to coincide with the presence of oxygen and hydrogen (Graph 4). As displayed by Graph 5, these elements are present both inside and outside the superficial film of sulfur and to the interface between film and sub-layer. The GDOES analysis also indicates that, in the first superficial layers, the copper content is higher if compared to the nominal composition of the sample (peak at 0,35 seconds at the same time of the sulfur's 1 second). This might have little influence on the growth kinetic of the tarnish film and therefore the correlated discoloration. In Graph 6 you can see Sample 1 undergoing oxidation at high temperature; at first it is possible to notice the presence of an elevated quantity of copper (higher than the nominal composition) in the first superficial layers. The increase in the concentration is concomitant to the reduction of the silver concentration. It is therefore assumed that the heat treatment leads to the generation of bi-phase structures inside the sample, related to the increase of the atomic mobility induced by the temperature. On this sub-layer a very thick layer of Copper oxide formed. Moreover, we detected the presence of a very thin tarnish film containing silver, sulfur and hydrogen over this oxide layer. The analysis also indicates that diffusion of oxygen and hydrogen took place inside the sample during heat treatment.

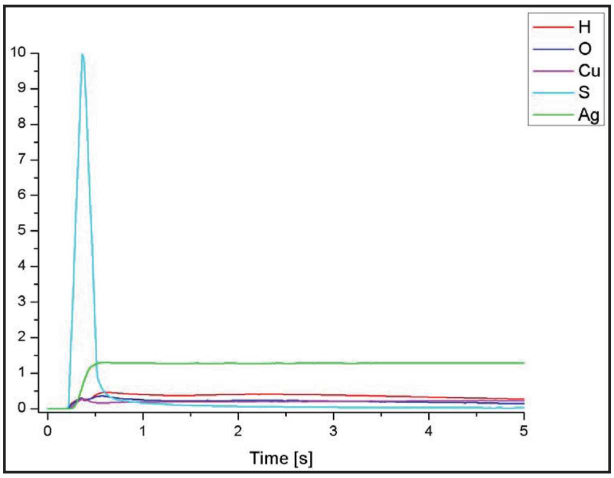

Graph 4 - GDOES analysis of sample 1 after sulfuration test

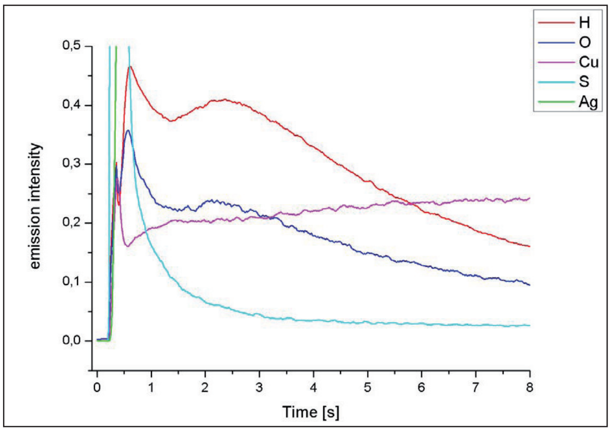

Graph 5 - – Zoom of the GDOES analysis of Sample 1 after sulfuration test

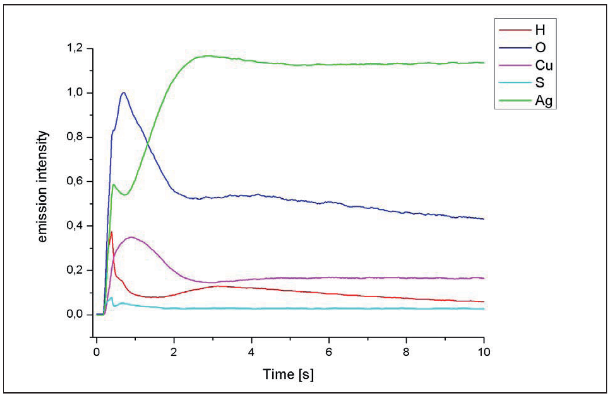

Graph 6 - GDOES analysis of Sample 1 after oxidation

Sample 2 also displays a superficial absorption of oxygen, hydrogen and sulfur (Graph 7). During Xenotest this sample evidenced a superficial layer of sulfur and sulfur derivates (Graphs 8 and 9). It is also possible to notice the presence of oxygen and hydrogen under this tarnish layer.

The pure silver sample in the sulfuration test displays an elevated concentration of sulfur in the first superficial layers as reported in Graph 10. The presence of sulfur is concomitant however with the presence of small traces of oxygen and hydrogen. The pure silver sample, after oxidation test, evidenced a very thick oxide layer in which you can observe impurities of oxygen and sulfur, usually present in the earth's atmosphere. It is worth nothing that the presence of oxygen inside the sub-superficial layers of the material is higher compared to the same samples after different tests (Graphs 11 and 12).

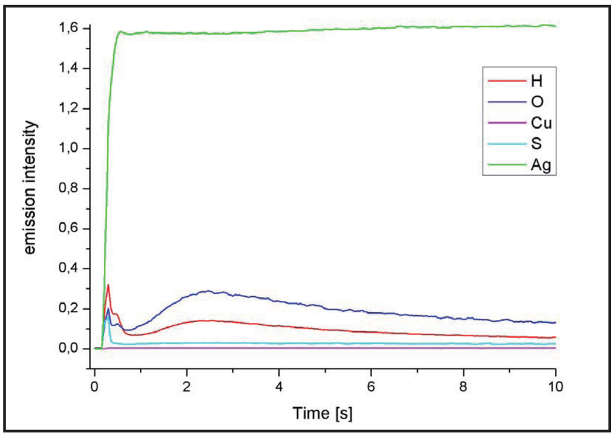

Graph 7 - GDOES analysis of Sample 2

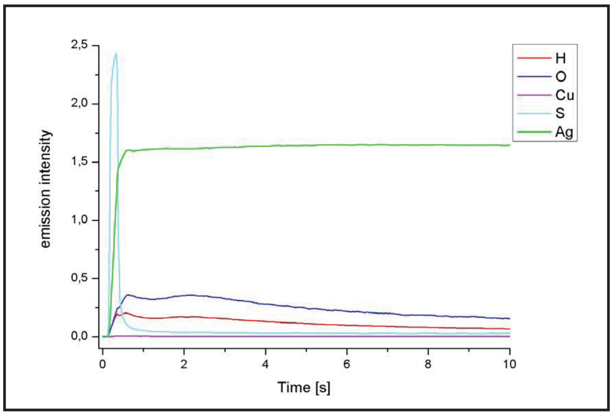

Graph 8 - GDOES analysis of Sample 2 after Xenotest

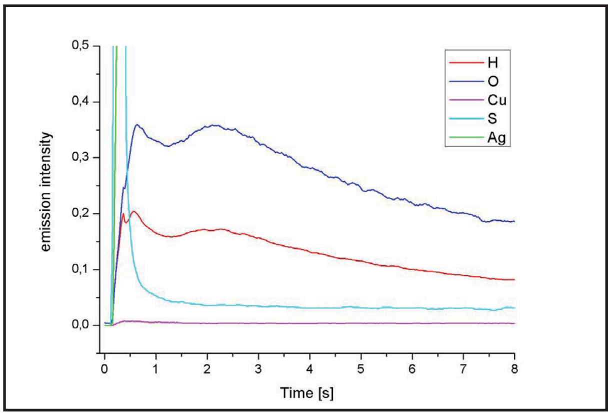

Graph 9 – Detail of the GDOES analysis of sample 2 after Xenotest

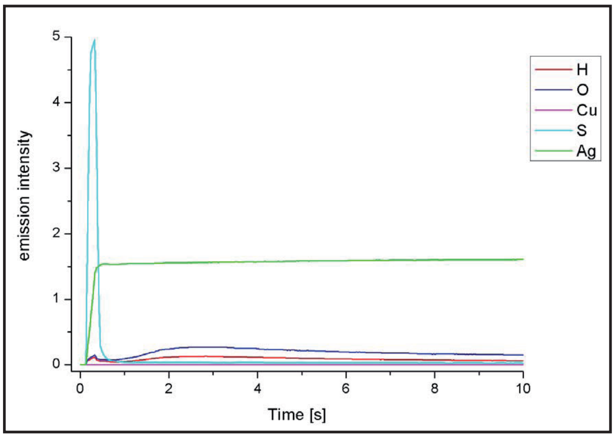

Graph 10 – GDOES analysis of sample 2 after sulfuration test

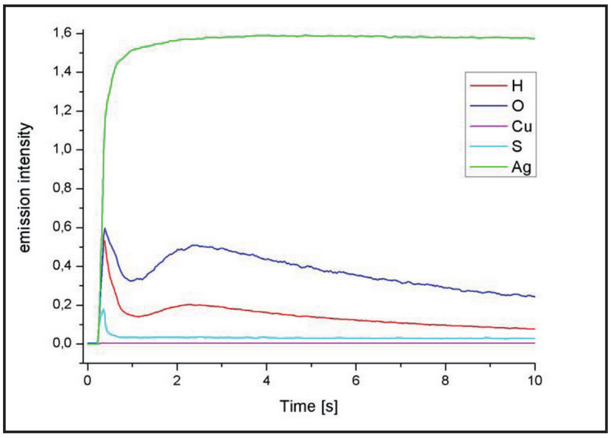

Graph 11 – GDOES analysis of sample 2 after oxidation test

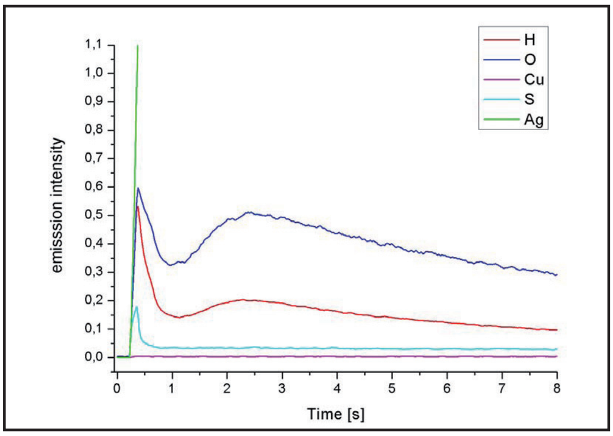

Graph 12 – Detail of the GDOES analysis of sample 2 after oxidation test

By the analysis of Sample 4 (Graph 13) it is evident that the surfaces are contaminated by the presence of sulfur in conjunction with a thin chemiosorbated or physisorbated layer of humidity a couple of hours after polishing.

In the analysis carried out on Sample 4, after several different tests it is possible to notice the absence of humidity films between the sub-layer and the tarnish film that is characteristic in previous Samples 1, 2 and 3 (Graphs 14 - 18).

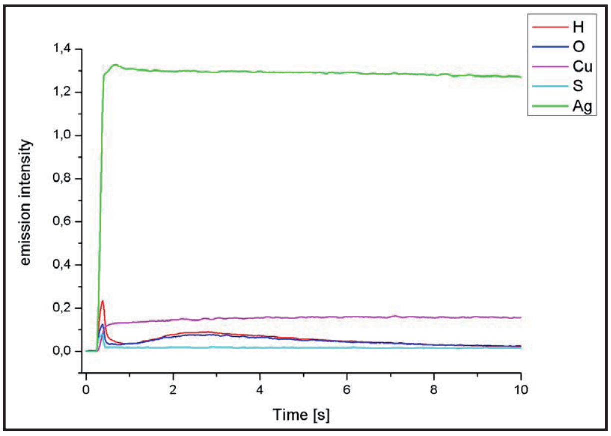

Graph 13 - GDOES baseline analysis of Sample 4

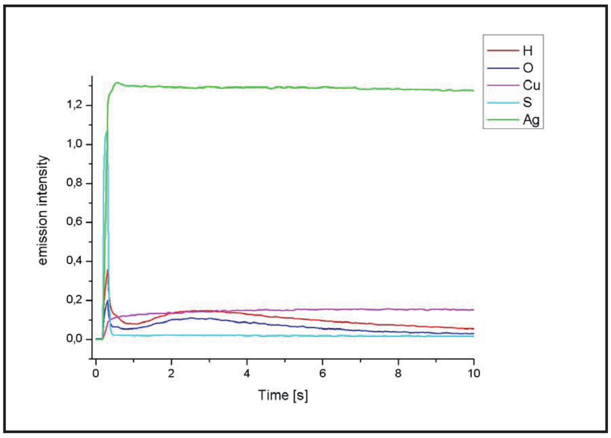

Graph 14 - GDOES analysis of Sample 4 after Xenotest

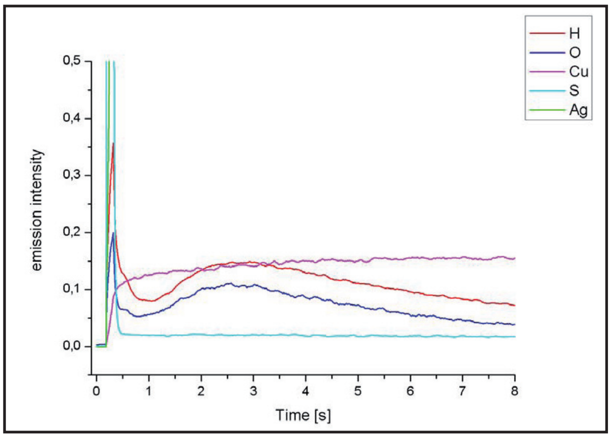

Graph 15 – Detail of the GDOES analysis of Sample 4 after Xenotest

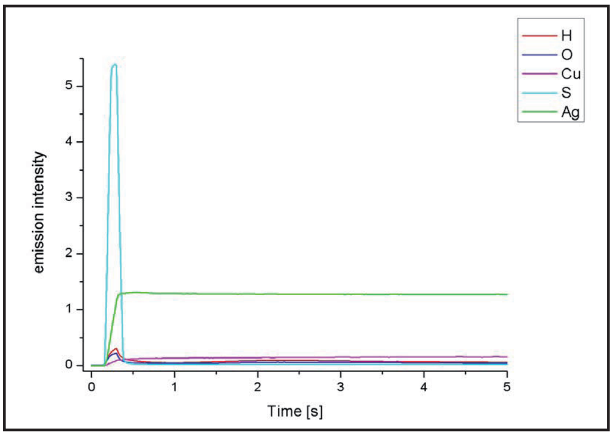

Graph 16 - GDOES analysis of Sample 4 after sulfuration test

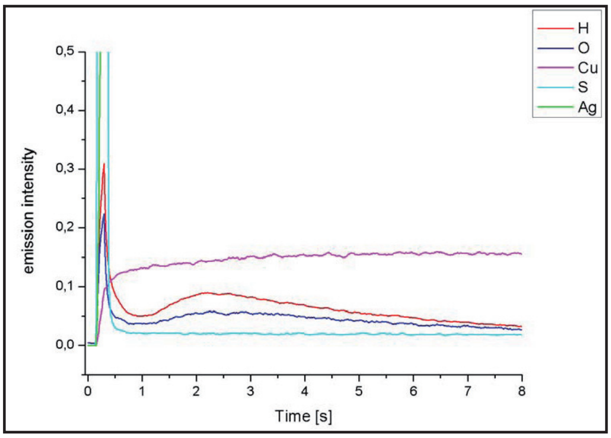

Graph 17 – Detail of the GDOES analysis of Sample 4 after sulfuration test

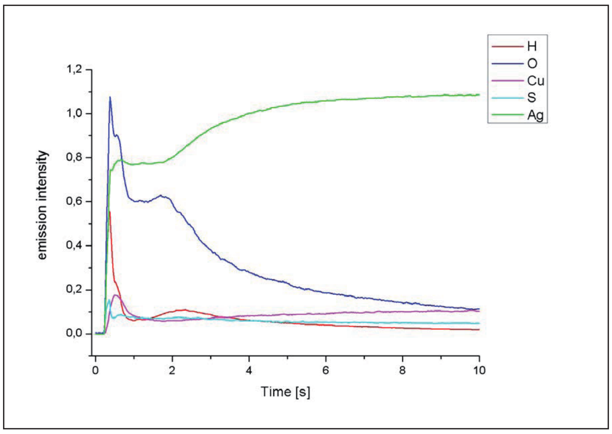

Graph 18 – GDOES analysis of Sample 4 after oxidation test

The analysis of samples 3 displays very well the profile of the silver layer deposited on the surface by galvanic process. Inside the film there are significant quantities of oxygen, hydrogen and sulfur. In fact, a couple of days after the samples were lapped the sulfur had already diffused through the thickness of the silver film (Graph 19).

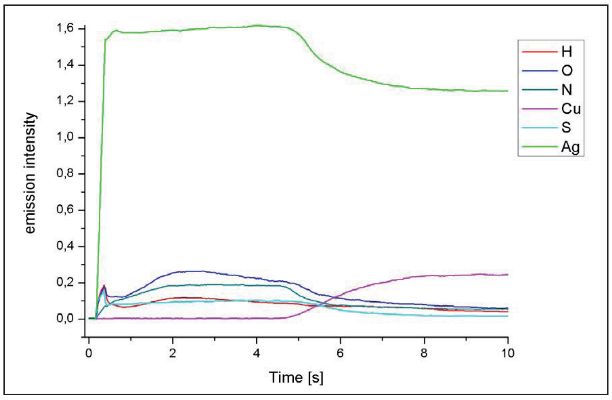

Graph 19 - GDOES analysis of the Silver plated sample used as "blank"

The presence of oxygen and hydrogen inside the deposited film is compatible with the SEM observations previously described.

Likewise, after the Xenotest Sample 3 displays a profile similar to the sample used as a baseline reference, i.e., the presence of sulfur and oxygen inside the silver film (Graphs 20 and 21). Graphs 22 and 23 report the analysis carried out on Sample 3 after the sulfuration test. Even after this test it is possible to notice, together with an elevated presence of sulfur on the first superficial layer, also its diffusion inside the sample. There are no significant considerations to make on Graph 24, related to Sample 3 after oxidation test.

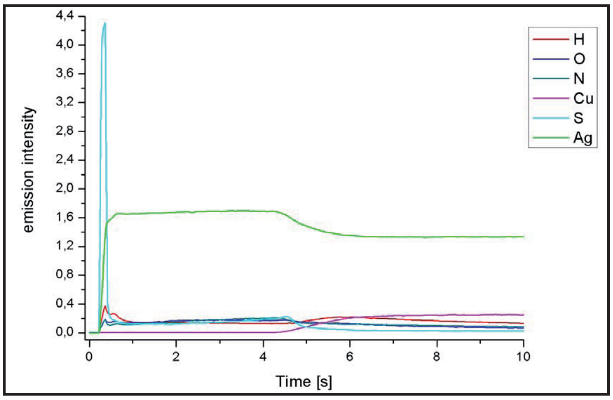

Graph 20 - GDOES analysis of Sample 3 after Xenotest

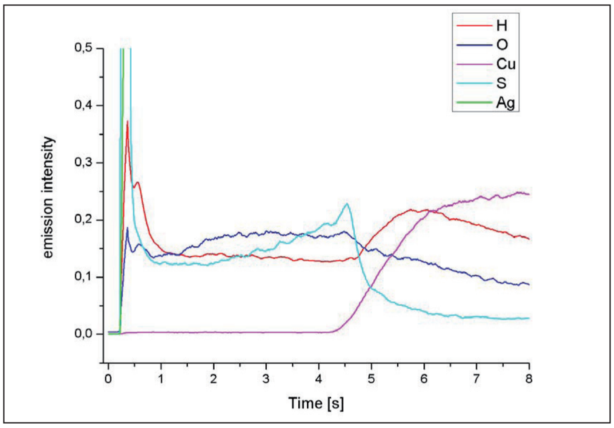

Graph 21 – Detail of the GDOES analysis of Sample 3 after Xenotest

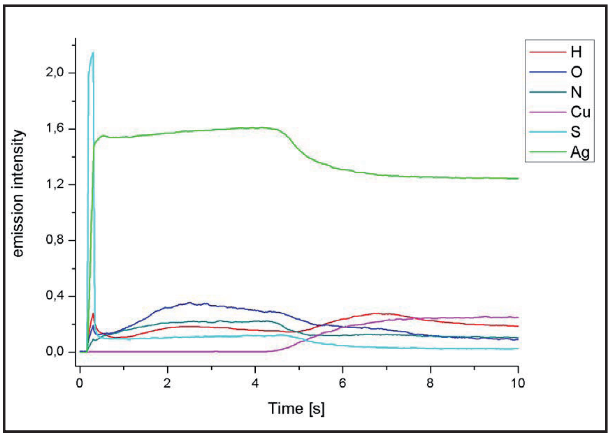

Graph 22 - GDOES analysis of Sample 3 after sulfuration test

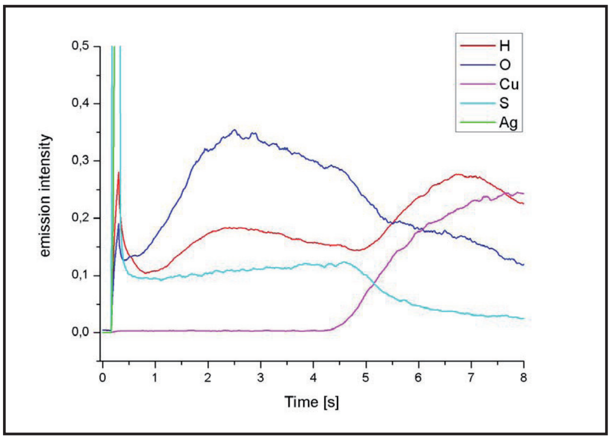

Graph 23 – Detail of GDOES analysis of sample 3 after Sulfuration test

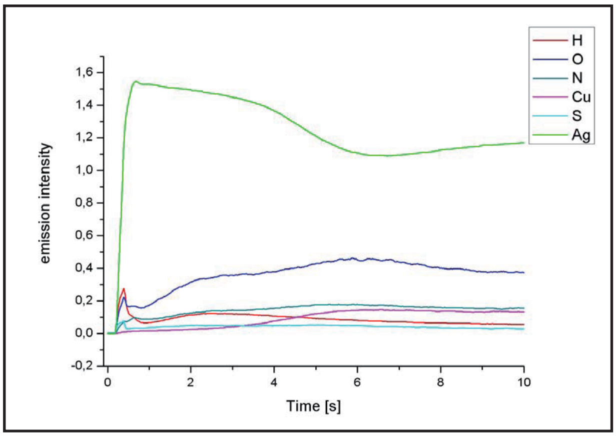

Graph 24 – Detail of the GDOES analysis of Sample 3 after oxidation test

Graph 25 reports the concentration of sulfur detected on the surface of the four samples after the sulfuration test. It is possible to notice that sample 4 has, on its surface, a sulfur concentration comparable to that of Sample 2 (pure silver). Graphs 26-28 show the concentration profiles for oxygen, hydrogen and copper.

For all the samples, the presence of oxides, hydroxides or sulfates was found on the first superficial layer. The presence of oxygen and hydrogen in the sub-superficial layers for Sample 1 is also evident, while the inside of Sample 4 displays a low concentration of these elements.

Graph 28 shows the presence of an elevated superficial concentration of copper in Sample 1. The high presence of this metal on the surface can induce dark discoloration of the piece since copper is easily oxidized. In addition to silver and copper sulfides, the concomitant presence of copper, oxygen and hydrogen atoms makes us believe that oxides, hydroxides and sulfates of copper are also present. The impressive discoloration of Sample 1 after sulfuration can be due to the presence on the surface of these compounds, too. The tarnish film after sulfuration can undertake bluish or purplish reflections that could be correlated to the fact that the superficial copper atoms undergo a complexation reaction and give birth to hydroxides and sulfates. The longer the exposure time is extended the more reddish the color becomes, which is connected to the further transformation of these compounds into copper oxides (I) with their typical reddish color.

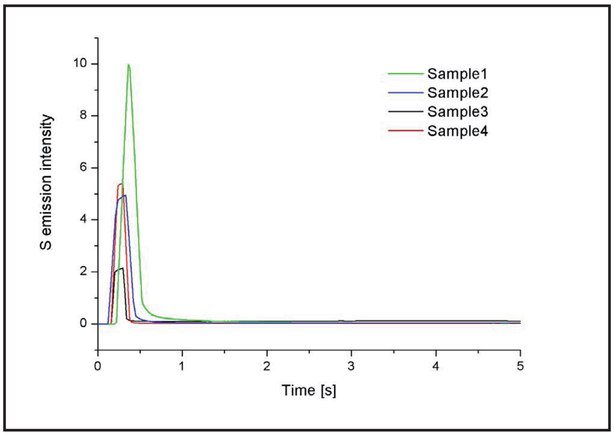

Graph 25 – Sulfur profile after sulfuration test

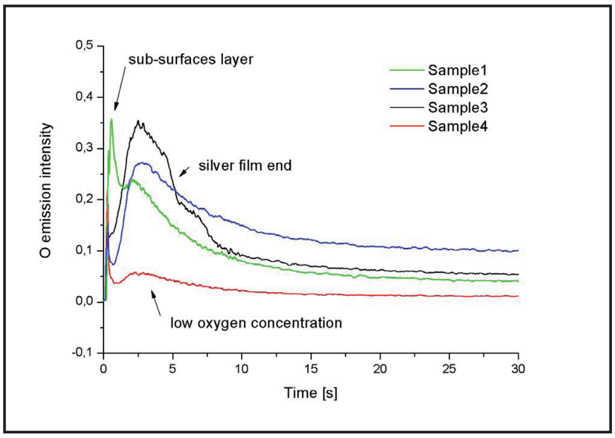

Graph 26 – Oxygen concentration profile after sulfuration test

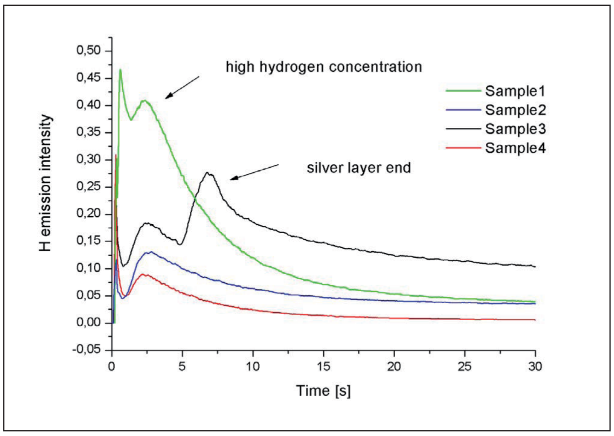

Graph 27 – Hydrogen concentration profile after sulfuration test

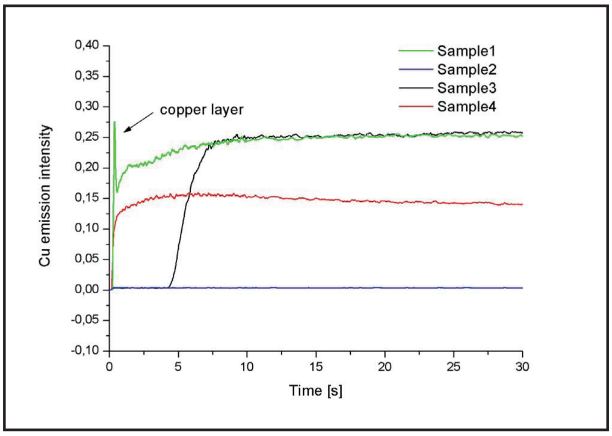

Graph 28 – Copper concentration profile after sulfuration test

Evidenced that the content of sulfur is higher for the samples where the content of superficial silver is higher (silver and silver plated) is shown by analysis of the Xenotest in Graphs 29-32. In fact, to the naked eye the color change is greater for these two samples when compared to Samples 1 and 4. The presence of humidity or hydroxides on the surface of the samples is also evident. It is possible that the relative humidity inside the Xenotest chamber is less compared to that generated during the sulfuration test. The concentration of water on the surface of the samples turns out to be minor and concurs to favor the sulfuration reaction on silver with regards to that of copper oxidation. However, the thickness of the superficial humidity layer has to be considered as a catalyst for both the reactions since it allows the reactant species to be in very close contact. The chemical reactions in the liquid state require less activation energy than for the gaseous state. This might explain the higher sulfur concentration on the surface of the samples with a higher silver concentration (Samples 2 and 3), as well as the discoloration data and the data obtained by the sulfuration trial for the sterling silver sample (Sample 1).

In conclusion, we find two different types of reactions. The first one is between sulfur and silver and the second one is between oxygen and copper. In addition, the possibility for the formation of copper sulfates and copper sulfites inside the tarnish film is evident.

Both the reactions cause some discoloration of the samples, but these are more marked when copper oxidation occurs due to the presence of humidity.

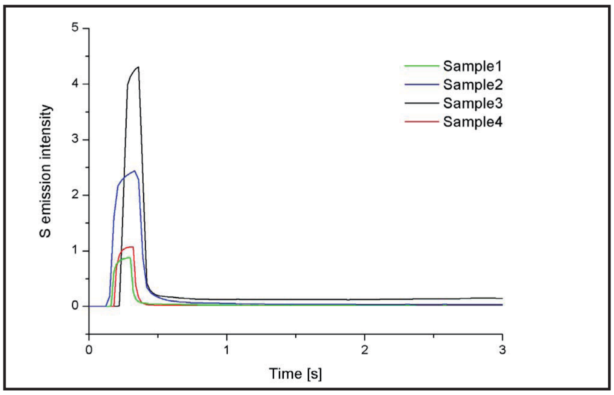

Graph 29 – Sulfur concentration profile after Xenotest

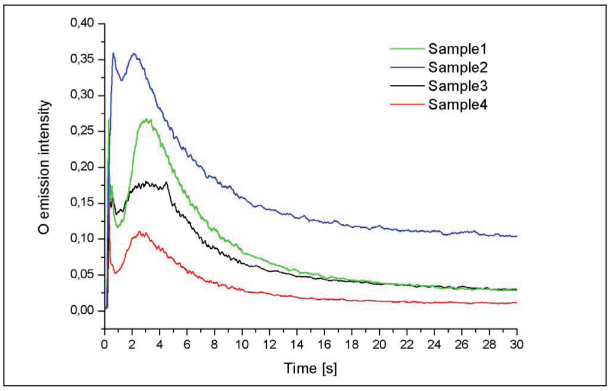

Graph 30 – Oxygen concentration profile after Xenotest

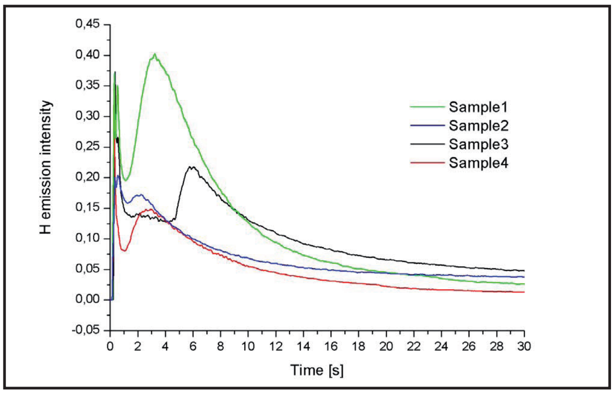

Graph 31 – Hydrogen concentration profile after Xenotest

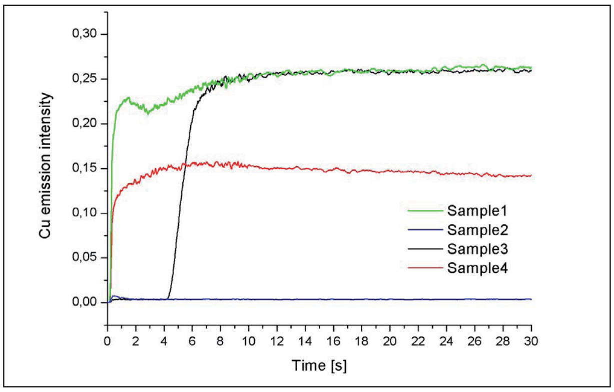

Graph 32 – Copper concentration profile after Xenotest

The GDOES analysis also detected concentrations of nitrogen, carbon, silicon and zinc. The first two, nitrogen and carbon, are impurities present inside the chamber where the plasma is generated and come from the external environment or by some argon gas contaminations. The concentration profiles for silicon and zinc, related to Sample 4, did not display particular trends; rather they showed a constant concentration all over the layer analyzed. For this reason we decided to omit this data from the graphs previously reported.

Concluding remarks

By comparing the data of the various tests we carried out, we can see that the resistance to tarnish depends in part on the type of test. In fact, comparing the data related to the sulfuration and the Xenotest, it is possible to see different behaviors for samples made of the same alloy. For example, if you consider Graphs 25 and 29, which report the sulfur concentration on the tested items, it is possible to see how Sample 1 (sterling silver) suffers a high aggression during the sulfuration test, while the same sample during Xenotest shows instead a behavior that turns out to be better if compared to Sample 2 (pure silver). In the same way, the samples containing a higher percentage of silver on their surface (Samples 2 and 3), demonstrated a good behavior during the sulfuration test, but during Xenotest, they suffered a more marked discoloration (Figures 5 and 9).

The tarnish reaction seems to be ruled by a complex mechanism, made of several chemical reactions (as supposed at the beginning of this paper), and as demonstrated through the temporal evolution of the colorimetric data collected during the Xenotest (Figures 8 and 9). So, the formation of a tarnish film and consequently the related discoloration are not only correlated to the reaction between sulfur and silver. Tarnish might therefore depend on many factors such as:

- The real content of silver on the surface;
- The presence of less noble elements, for example copper, that react readily with the polluting atmo-

spheric elements;
- The presence of elements such as silicon and zinc, which might grow inert oxides on the surface, limiting the concentration and the reactivity of other chemical species present in the alloy;
- The presence of a bi-phase structure that may generate micro-cells on the surface of the piece or could work as a trigger point for the reaction;
- The presence of a humidity film on the surface of the sample.

In addition to the above considerations, the presence of oxygen and hydrogen together with sulfur was detected in the GDOES analysis on the surface of the samples. This points to the possibility that the tarnish phenomenon involves sulfuration reactions and oxidation of other elements in the alloy, such as copper, as well as the sulfuration of silver. It is possible that the superficial variation of the color displayed by silver is not due exclusively to the silver sulfuration reaction, but that it also involves the formation of other chemical species.

The copper corrosion related to the direct contact with the atmosphere is very well known since that has been widely studied in past centuries. Copper not only forms a heavy oxides film on the surface when exposed to the atmosphere, it also reacts to form compounds with other polluting elements. At the beginning, oxygen and water react with copper to form a superficial layer like Cu2O/CuO/[Cu(OH)2 or CuO x H2O]; where the main reactant component is gas it would be (SO2, NO2, O3, Cl2, HCl and H2S). The main compounds you can find on the surface are therefore Cu2Cl(OH) 3, Cu4SO4 (OH)6.H2O, and in the urban areas, Cu4-SO4 (OH)x, e Cu2CO3(OH) 2 [6, 7, 8].

In the sulfuration trials related to Sample 1, it is possible that the superficial layer, at first glance connected exclusively with the superficial formation of sulfides, is in truth made mainly of cuprite (Cu2O), copper hydroxide (Cu(OH)2) and copper sulfates. We presume, in fact, that the surface discoloration is mainly due to the formation of such compounds and in part to the reaction of silver sulfuration. The visual analysis of this film is compatible with a structure as follows: Cu2O/[Cu(OH)2 or CuO x H2O].

During the sulfuration test, it is thought that the first is of cuprite. This reaction is favored by humidity depositing on the surface of the sample in the first minutes of test and the high concentration of oxygen in contact with the sample. The discoloration is therefore a function of the thickness of cuprite growth and may vary from yellow to reddish. Since the chamber is closed, the relative humidity inside ranges from 30-80%, keeping the samples quite most, and the complexation reaction between water and copper forms Cu(OH)2, with the typical azure color on the surface. This layer of hydroxide will form on the cuprite layer since it has a higher concentration of water molecules. This mechanism can therefore explain the visual analysis carried out on Sample 1 after sulfuration and reported in Figure 22.

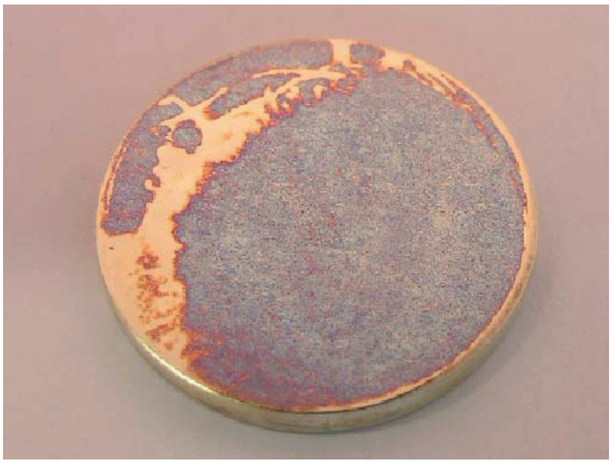

Figure 22 - Sample1 after sulfuration test: 40 minutes

This alloy is composed of silver and copper and as the SEM observations show, the superficial structure consistes of copper-rich phases alternating with silver-rich phases. The presence of the copper-rich material on the surface quickens the reaction, since it takes place mainly in the less noble zones on the pieces. Furthermore, the presence of sulfuric acid inside the chamber provides an acid environment that activates the oxidation and complexation reaction of Copper.

The compositional variation on the surface of each single sample analyzed is responsible for the lack of colorimetric measurement repeatability since the content of copper in touch with the external environment is very important and controls the speed of the reaction. The speed of copper oxide formation is preponderant when compared with that if copper sulfide formation. We do not exclude, however, the formation of copper sulfates to the detriment of the sulfides.

Silver sulfuration takes place parallel to the copper oxidation, but this does not seem to depend in such an evident way on the relative humidity, like the reaction involving copper. In fact, Samples 2 and 3 have much less variation of discoloration than Sample 1, due to the homogeneity on the surface. With Samples 2 and 3 you can notice that the color variations correlate with the superficial finishing of the samples. In fact, by the GDOES analysis (Graphs 20 and 21) it is possible to notice how sulfur underwent diffusion phenomenon inside the silver film during Xenotest, maybe connected to the higher temperature caused by the incident light radiations, which might have degraded the coating film, making possible the diffusion of polluting elements from the atmosphere.

The behavior of Sample 4 so is compatible with this theory, since the silver is very concentrated in the composition of the surface to the detriment of copper. Conversely, the tarnish process is accelerated on sterling silver due to the bi-phase structure, as seen in the SEM analysis of Sample 1. However, zinc and silicon can work as sacrificial elements if they are present in sufficient concentrations to inhibit the oxidation process of copper.

It was stressed how the content of copper in the samples plays a fundamental role in the tarnish phenomena. With the data in our possession, it is difficult to unequivocally correlate the concentration of silver on the surface with the content of sulfur present in the tarnish film for different tests. First it should be necessary to repeat the sulfuration and Xenotest, trying to equalize the concentration of pollutants in the chamber to discover the dependence of the copper concentration in the samples on the relative humidity and the incident radiation. This means studying a new experimental set-up for the sulfuration test and therefore for the Xenotest as well. It might also be helpful to improve the calibration method of the GDOES spectrophotometer, by which it may be possible to have a certain correspondence between the intensity of emission of the elements and their concentration on the surface. Last but not least, an estimation of the sputtering range is needed in order to calculate the thickness and consequently the rate of growth of the film itself.

With the data in our possess it may be possible to think about characterizing the whole reaction mechanism and the growth of the tarnish film in order to be able, in a further step, to analyze the role played by each chemical element introduced in the sample, as well as, thanks to the use of a colorimeter, to find out a simple method to estimate the real life of a sample by the analysis made in the laboratory.

To our point of view, the use of sulfuration test is not adequate to evaluate the effective tarnish resistance of silver alloy samples because it is not possible to have an accurate control of some parameters involved in the complex chemistry of the tarnish process. We speculate that to adequately study the tarnish process, new test equipment should be devised that controls the temperature and relative humidity inside the reaction chamber. The tarnish test should also allow the introduction of gas mixes containing known values of polluting elements, such as sulfur and chlorine, etc. The control of such parameters helps to fully understand the mechanism ruling this phenomenon and evaluate the kinetic of the reaction.

The use of a spectrophotometer to evaluate the discoloration of the samples seems to be a good choice. It allows sufficiently small incremental measurements of the colorimetric coordinates L*, a* and b* as well as the most important, which is vector ΔE. As mentioned before, the use of a Xenotest fulfilled the need for simulating what happens to silver items in shops windows. Although the Xenotest instrument has a temperature check and the ability to regulate and control the relative humidity, it unfortunately does not allow polluting gases to be introduced inside.

10. Acknowledgments

ProGold's R&D Laboratory would like to thank Dr. Simone Vezzù of the CIVEN (Venetian Interuniversity Coordination for Nanotechnologies), Marghera, Venice, for his collaboration and promptness in carrying out the analysis.

11. Bibliography

1. J.I. Lee, J.J. Howard, W. Kellar, W. Cross and K.N. Han, "Electrochemical Interaction between Silver and Sulfur in Sodium Sulfide Solutions", Metallurgical and Materials Transactions B, Volume 32B (2001): 895.
2. E. Ramous, "Il problema dell'annerimento dell'argento: perché accade e quail le modalità di valutazione del fenomeno", Jewellery Technology Forum (2005): 259-270.
3. L. Gal-Or, "Tarnish and Corrosion od Silver and Gold Alloys", The Santa Fe Symposium on Jewellery Manufacturing Technology 1990, ed. Dave Schneller (Boulder, Colorado: Met-Chem Research, 1990).
4. G.M. Ingo and I. Calliari, "Combinated use of GDOES, SEM+EDS, XRD and OM for the microchemical study of the corrosion products on archaeological bronzes", Applied Physics A 79 (2004): 199-203.
5. I. Calliari and G.M. Ingo, "Microchemical study of the corrosion products on ancient bronzes by means of glow discharge optical emission spectrometry", Surface and Interface Analysis 30 (2000): 264-268.
6. S. Syed, "Atmospheric Corrosion of Materials", Emirates Journal Engineering Research 11, 1 (2006): 1-24.
7. ASM Handbook, Vol. 13, Corrosion
8. D.J. De Renzo, Corrosion Resistant Materials Handbook, Fourth Edition (1985).